Bioorganic & Medicinal Chemistry 19 (2011) 2659–2665

Contents lists available at ScienceDirect

Bioorganic & Medicinal Chemistry

journal homepage: www.elsevier.com/locate/bmc

Inhibitors and promoters of tubulin polymerization: Synthesis and biological evaluation of chalcones and related dienones as potential anticancer agents

Christine Dyrager [a], Malin Wickström [b], Maria Fridén-Saxin [a], Annika Friberg [a], Kristian Dahlén [a], Erik A. A. Wallén [a,c], Joachim Gullbo [b], Morten Grøtli [a], Kristina Luthman [a,*]

[a] Department of Chemistry, Medicinal Chemistry, University of Gothenburg, SE-412 96 Göteborg, Sweden
[b] Division of Clinical Pharmacology, Department of Medical Sciences, Uppsala University Hospital, SE-751 85 Uppsala, Sweden
[c] Division of Pharmaceutical Chemistry, Faculty of Pharmacy, University of Helsinki, FI-00014 University of Helsinki, Finland

ARTICLE INFO

Article history:
Received 30 November 2010
Revised 27 February 2011
Accepted 3 March 2011
Available online 10 March 2011

Keywords:
Chalcones
Cytotoxicity
Tubulin polymerization
Molecular modeling

ABSTRACT

A series of dihalogenated chalcones and structurally related dienones were synthesized and evaluated for their antiproliferative activity in 10 different cancer cell lines and for their effect on microtubule assembly. All compounds showed cytotoxic activity, with IC_{50} values in the 5–280 μM range depending on the chalcone structure and the cell line. Five of the compounds were found to be tubulin polymerization inhibitors. In contrast, one of the compounds was found to stabilize tubulin to the same extent as the anticancer drug docetaxel. Molecular modeling suggested that the tubulin inhibitors bind to the colchicine binding site of β-tubulin while the novel tubulin stabilization agent seems to interact with the paclitaxel binding site.

1. Introduction

Chalcones (Fig. 1) are naturally occurring compounds acting as intermediates in the biosynthesis of flavonoids, which are of interest due to their wide range of biological activities. Chalcones are also pharmacologically active and have been shown to act as antimitotic,[1] antiproliferative,[2] anti-inflammatory,[3] and antiviral agents.[4,5] Due to their anticancer activities, considerable efforts have been dedicated to identify new potential chalcone-based drug candidates within the oncology field.[6] Their cytotoxic activity is often associated with tubulin inhibition and the ability of interfering with microtubule formation, which is essential in cellular processes such as mitosis, cytoplasmic organelle movement, cell replication, and for regulation of cell shape.[7]

In general, antimitotic agents act by targeting three different sites on the tubulin heterodimer: the colchicine, the vinca alkaloid and the paclitaxel binding sites (Fig. 2). Agents that bind to the colchicine binding site (e.g., colchicine and podophyllotoxin) or to the vinca alkaloid domain (e.g., vincristine) are defined as inhibitors of tubulin assembly, that is, microtubule destabilizing agents. On the contrary, agents that target the paclitaxel binding site (e.g., paclitaxel or docetaxel) are known to act as tubulin promoters, that is, microtubule-stabilizing agents (Fig. 3).[8]

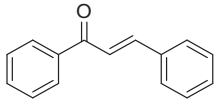

Figure 1. The general structure of chalcones.

Several chalcones have been reported to act as cytotoxic agents or as microtubule destabilizing agents, targeting the colchicine binding site.[1,7,9,10] The majority of these are naturally occurring compounds substituted with electron donating hydroxy and/or methoxy groups at various positions.[5,7,11–13] To establish more advanced structure–activity relationships around chalcones, the synthesis of compounds with more diverse substitutions patterns is of great importance. In our research aiming at the development of novel scaffold-based peptidomimetics, various dihalogenated chalcones have been of interest as intermediates in the synthesis of flavones and chromones.[14,15] Such halogenated chalcones have been reported to exhibit high cytotoxic activities.[16]

Herein, we report the synthesis of a series of chalcones and related dienones synthesized from two structurally similar electron-poor dihalogenated 2′-hydroxyacetophenones and aryl aldehydes with electron withdrawing or donating substituents in the *para*-position. The synthesized compounds were evaluated for their

* Corresponding author. Tel.: +46 31 7869031; fax: +46 31 7723840.
E-mail address: luthman@chem.gu.se (K. Luthman).

0968-0896/$ - see front matter © 2011 Elsevier Ltd. All rights reserved.
doi:10.1016/j.bmc.2011.03.005

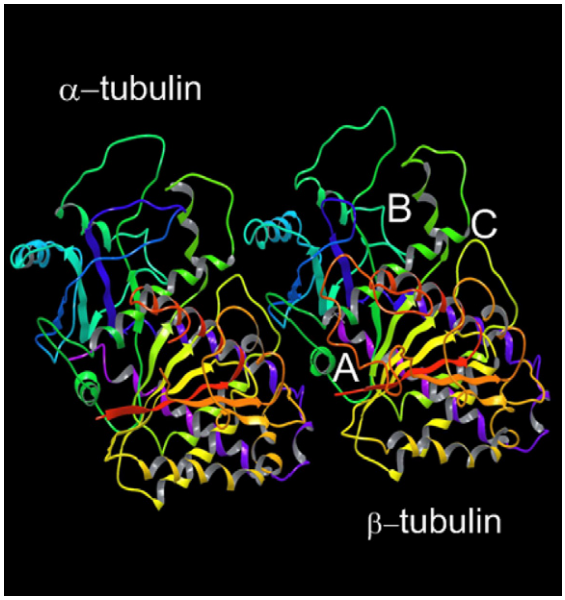

Figure 2. Illustration of the tubulin α,β-heterodimer with three major binding sites on β-tubulin; the colchicine binding site (A), the paclitaxel binding site (B), and the vinca alkaloid domain (C).

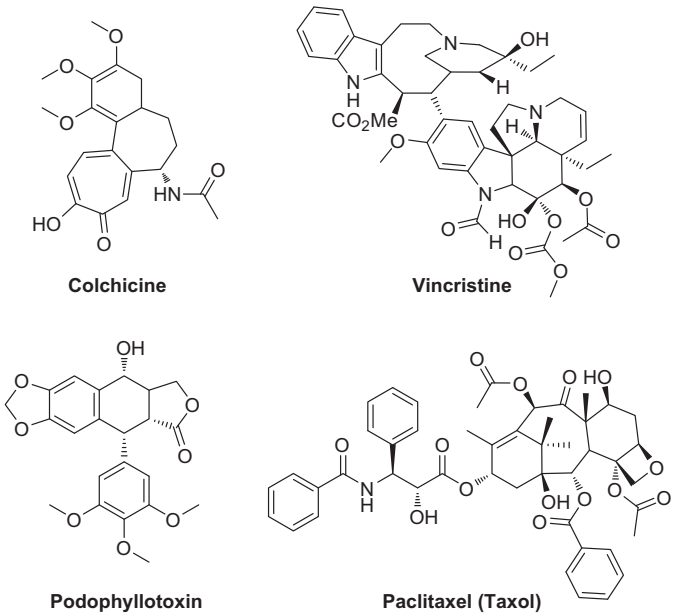

Figure 3. Chemical structures of known tubulin inhibitors (colchicine, vincristine, and podophyllotoxin) and paclitaxel, a promoter of microtubule assembly.

cytotoxic activity towards 10 different cancer cell lines. They were also investigated for their activity in a microtubular polymerization assay. All compounds showed cytotoxic activities, most of them were also found to act as either tubulin inhibitors or promoters. In addition, computer-based docking studies have been performed in an attempt to rationalize the biological results.

2. Results and discussion

2.1. Synthesis

Chalcones **1**–**2** were synthesized in high yields via an aldol condensation of a 3′,5′-dihalogenated-2′-hydroxyacetophenone

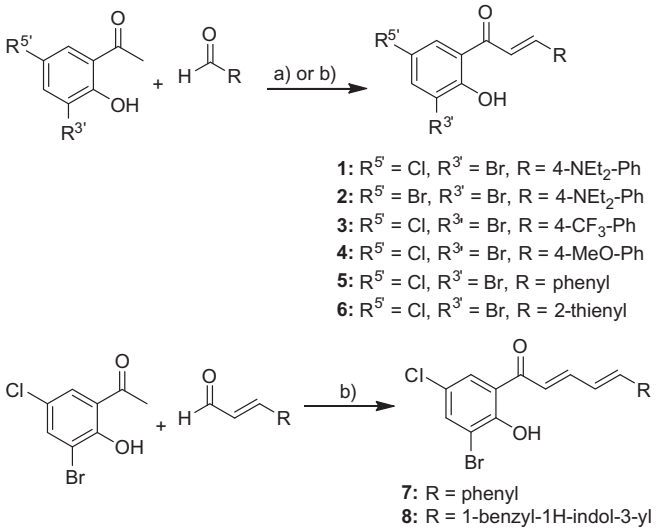

Scheme 1. Synthesis of chalcones **1**–**6** and dienones **7**–**8**. Reagents and conditions: (a) NaOH (aq) (60%), MeOH, room temperature, overnight; (b) KOH, EtOH, 50 °C → room temperature, overnight.

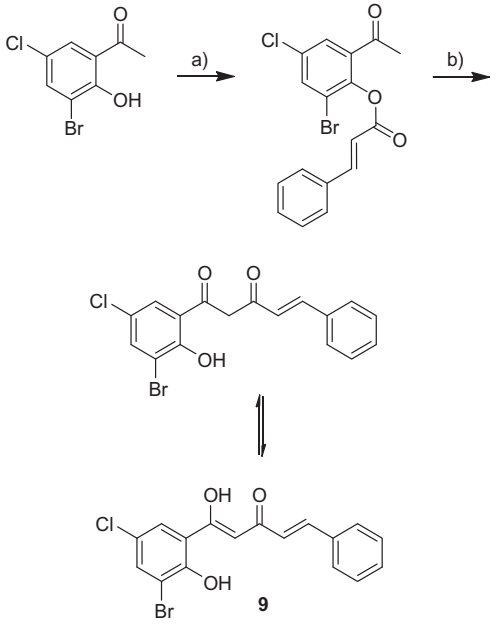

Scheme 2. Synthesis of compound **9**. Reagents and conditions: (a) *trans*-Cinnamoyl chloride, pyridine, room temperature, 48 h; (b) K_2CO_3, 2-butanone, reflux, 3.5 h.

and 4-diethylaminobenzaldehyde using aqueous NaOH (60%) in MeOH (Scheme 1).[15,17] Less alkaline conditions, KOH in EtOH, were used for the synthesis of chalcones **3**–**6** and dienones **7**–**9** from 3′-bromo-5′-chloro-2′-hydroxyacetophenone and the appropriate aldehyde (Scheme 1).[14] Compound **9** was prepared in two steps from 3′-bromo-5′-chloro-2′-hydroxyacetophenone via esterification with benzoyl chloride followed by an intramolecular Baker–Venkataraman rearrangement (Scheme 2).[18] Interestingly, NMR spectroscopy revealed that **9** exists as an enol tautomer.

2.2. Biological characterization

2.2.1. Cytotoxicity studies

Compounds **1**–**9** were tested for their cytotoxic effect against 10 different human cancer cell lines (Table 1) using a fluorometric

Table 1
Cytotoxicity of chalcones **1**–**6** and dienones **7**–**9** against 10 cancer cell lines determined using the FMCA method.

Compd	Cytotoxicity, IC_{50} (μM)									
	CCRF-CEM	CEM/VM1	ACHN	U937-GTB	U973/Vcr	RPMI 8226	8226/Dox40	8226/LR5	NCI-H69	H69AR
1	14.8	14.5	164[a]	9.3	8.8	29.4	9.7	9.4	5.2	24.5
2	20.1	13.1	69[a]	8.2	9.6	26.1	7.7	9.9	7.1	38.8
3	15.4	31.1	49.4	14.9	24.4	20.8	22.5	22.3	11.5	33.2
4	111[a]	45.8	49.4	45.0	77[a]	80[a]	16.9	46.0	16.4	42.6
5	37.6	22.3	48.9	20.0	24.2	18.7	12.4	13.2	10.3	26.4
6	152[a]	48.9	44.2	42.5	32.6	79[a]	26.5	23.3	20.0	56.1
7	129[a]	48.6	93[a]	36.6	31.7	48.8	14.2	23.4	19.9	N.D.[b]
8	280[a]	89[a]	17.0	49.0	54[a]	119[a]	42.3	70[a]	11.1	48.5
9	34.1	24.1	37.8	18.1	23.9	27.9	19.1	33.5	9.4	25.5

[a] Extrapolated values (highest tested concentration of 50 μM).
[b] Not determined (no cytotoxic effect was observed).

microculture cytotoxicity assay (FMCA).[19,20] The results, summarized in Table 1, showed that all compounds exhibit cytotoxic activities with observable variations due to structural differences. Compounds **1** and **2** showed similar activity profiles, with the highest activity against the NCI-H69 cell line (IC_{50} 5.2 and 7.1 μM, respectively). The difference in cytotoxicity between **1** and **2** in the renal adenocarcinoma cell line (ACHN) (IC_{50} 164 and 69 μM, respectively) suggests that ACHN is sensitive to size changes in the 5′-position of these chalcone derivatives. When comparing **3** and **4** (4-CF_3-phenyl vs 4-MeO-phenyl) the electron donating 4-methoxy group was unfavorable in three of the tested cell lines: CCRF-CEM, U973/Vcr, and RPMI 8226. This result is more likely due to the difference in size between the trifluoromethyl and the methoxy group than the difference in electronic properties since the cytotoxic activity of **5** (no substituent on the phenyl group) is similar to that of **3**. Furthermore, the 2-thienyl derivative **6** showed decreased activity in several of the cell lines when compared with the slightly larger bioisosteric phenyl derivative **5**, most noticeable in CCRF-CEM (IC_{50} 152 vs 37.6 μM). Elongation of the carbon chain between the aromatic moieties in **5** to obtain **7** also resulted in decreased activities. However, the introduction of a dienone fragment as in **9** improved the activity with IC_{50} values corresponding to that of **5**. Furthermore, introducing an additional aromatic moiety, such as in **8**, gave low activity in several of the tested cell lines, for example, CCRF-CEM (IC_{50} 280 μM), while a higher activity was observed toward the small-cell lung cancer cell line (NCI-H69) (IC_{50} 11.1 μM). In addition, **8** showed the highest activity among the tested compounds toward the ACHN cell line (IC_{50} 17.0 μM), known for its aggressive and high resistance profile.[21]

One potential mechanism of cytotoxicity could be that the chalcones act as electrophiles in Michael reactions.[22] To investigate this hypothesis we tested the reactivity of the chalcones using glutathione as a nucleophile. No glutathione conjugate was formed (data not shown) indicating that that the observed activity of the chalcones is not due to the reactivity of the α,β-unsaturated carbonyl moiety.

2.2.2. Tubulin polymerization assay

The tubulin polymerization activity of compounds **1**–**9** is summarized in Figure 4. Compounds **3**, **4**, and **9** revealed no significant influence on tubulin assembly, which suggests a different mechanism for the observed cytotoxicity than tubulin inhibition (Table 1). However, five compounds (**1**, **2**, **5**, **6**, and **7**) showed significant inhibition of tubulin assembly. In contrast, chalcone **8** displayed microtubule-stabilizing activity comparable to the well-established antimitotic chemotherapeutic drug docetaxel, which is used in the treatment of several types of cancer.[23] To the best of our knowledge, compound **8** is the first reported chalcone with microtubule-stabilizing activity.

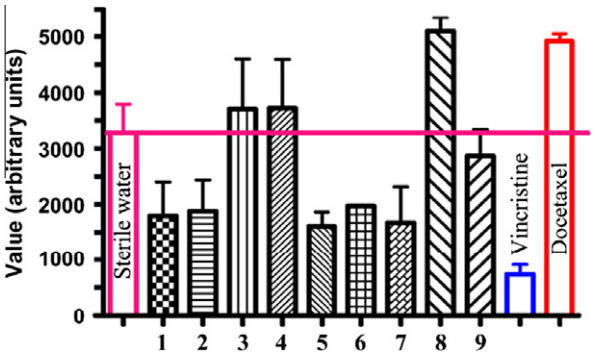

Figure 4. Tubulin polymerization activity in the presence of compound **1**–**9** (25 μM, mean values from duplicates of each experiment are presented) with vincristine and docetaxel (3 μM) as reference compounds. Stacks below the horizontal (pink) line indicate tubulin inhibition, stacks above indicate tubulin stabilization and stacks close to the horizontal line are considered to represent inactive compounds. The *y*-axis demonstrates tubulin polymerization activity measured at 15 min (arbitrary units) in the growth phase of the tubulin polymerization curve.

2.3. Molecular modeling

Molecular modeling was performed in order to explore possible binding modes for the compounds that showed activity toward tubulin polymerization (Fig. 4). The microtubule destabilizing compounds **1**, **2**, **5**, **6**, and **7** were docked into the colchicine binding site of tubulin using the podophyllotoxin-tubulin complex (PDB 1SA1) as template.[24,25] Podophyllotoxin binds into a hydrophobic pocket on β-tubulin that contains two hydrophobic centers; one surrounded by Metβ259, Alaβ316, and Lysβ352 (occupied by the benzodioxole fragment in podophyllotoxin), and one surrounded by Leuβ242, Alaβ250, and Leuβ255 (occupied by the trimethoxyphenyl moiety) (Fig. 5A).[26] In this study we observed that chalcones **5** (Fig. 5B) and **6** bind to the colchicine binding site by directing the phenyl or 2-thienyl moieties, respectively, into the benzodioxole binding pocket. Furthermore, the 3-bromo-5-chloro-2-hydroxyphenyl moiety could fit into the other hydrophobic pocket. However, compounds **1**, **2**, and **7** are more elongated and are not able to adopt a conformation that utilizes both these hydrophobic sites. Instead, the styryl group in **7** is directed out from the binding site and positioned on the surface of the binding pocket. However, tubulin activity is not lost since the 3-bromo-5-chloro-2-hydroxyphenyl moiety is located in the same hydrophobic area as the corresponding moiety in chalcone **5** (Fig. 5B) and it is actually buried deeper inside the pocket and thereby utilizes the area more efficiently. In contrast, compounds **1** and **2** (Fig. 5C) bind in a flipped fashion; the 4-diethylaminophenyl group

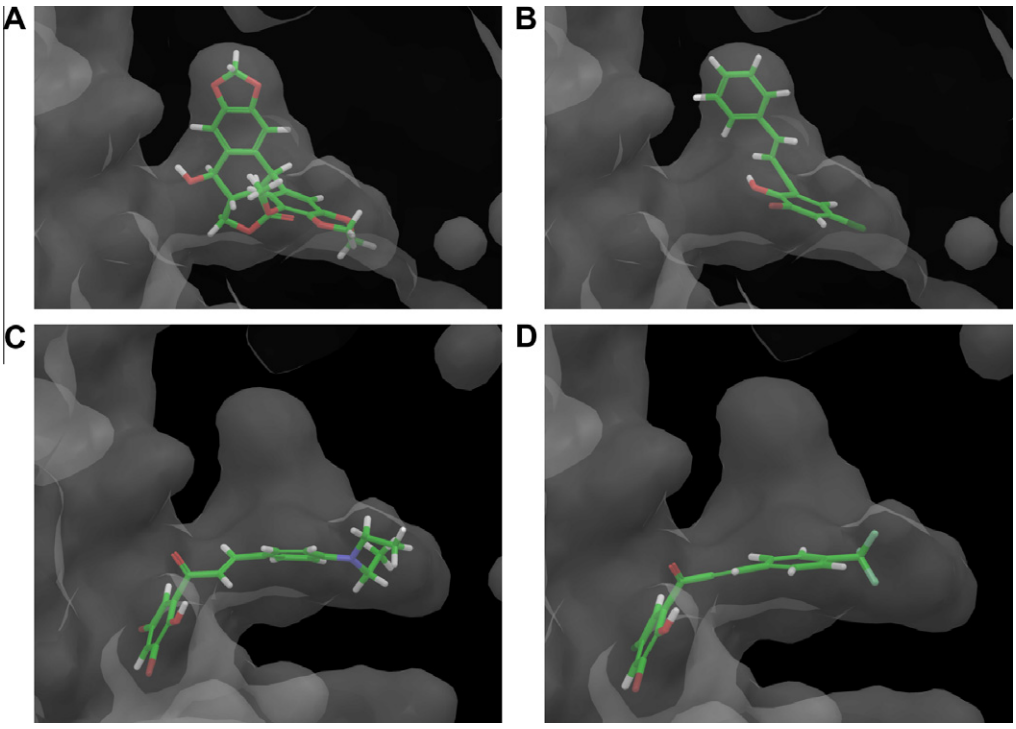

Figure 5. Examples from the docking study into the colchicine binding site of β-tubulin: (A) podophyllotoxin, (B) the tubulin inhibitor **5** (the carbonyl group is not visible in the illustration as it is hidden behind the carbon skeleton), (C) the tubulin inhibitor **2**, and (D) the inactive compound **3**.

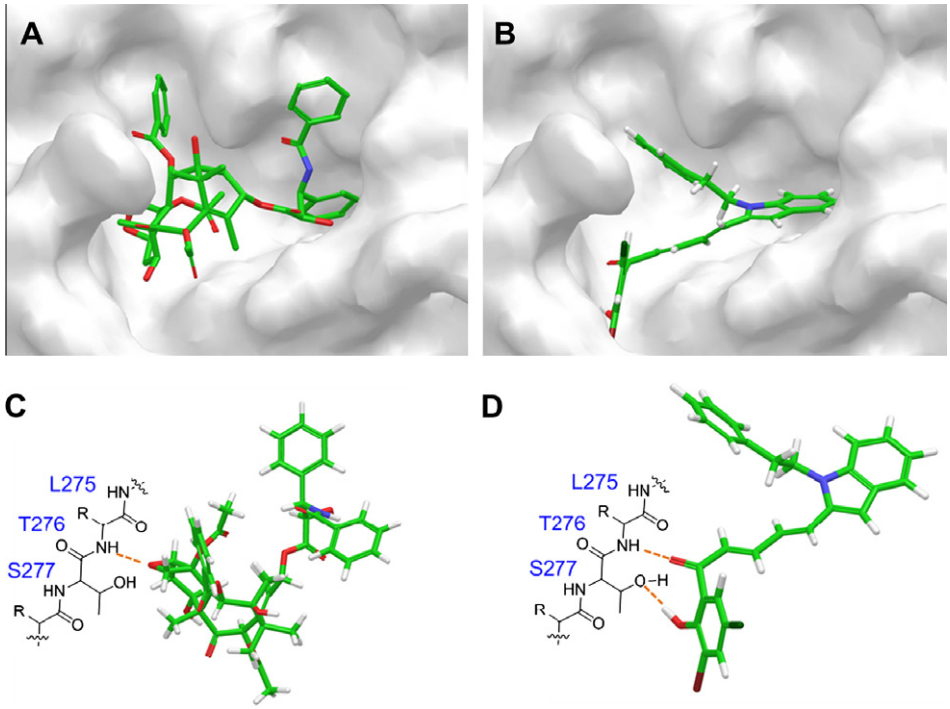

Figure 6. Comparison of paclitaxel (A) and compound **8** (B) docked in the paclitaxel binding site of tubulin. Panels C and D show potential hydrogen bonding interactions (orange dashed lines) between paclitaxel or **8** and Thr276 in the active site of the tubulin heterodimer.

is instead placed into the trimethoxyphenyl pocket and the rest of the molecule is directed outwards from the active site. The inactive compounds, **3** (Fig. 5D), **4** and **7,** were also docked into the colchicine binding site of tubulin. Interestingly, **3** and **4** adopt the same flipped binding mode as **1** and **2** but the trifluoromethyl or the methoxy group is not able to achieve contact with the hydrophobic pocket to the same extent as the diethylamino moiety in **1** and **2**. Furthermore, compound **9** was positioned in a similar manner as **5** (Fig. 5B) but the 3-bromo-5-chloro-2-hydroxyphenyl moiety was shown to adopt a slightly different angle and could

therefore not reach as far into the pocket as the corresponding moiety in **5**.

The microtubule-stabilizing compound **8** was docked into the paclitaxel binding site of β-tubulin using the paclitaxel-tubulin crystal structure (PDB 1JFF).[24,27] The large and complex structure of paclitaxel binds to tubulin through multiple hydrophobic interactions (Fig. 6A). The phenyl ring of the 2-benzoyl ester moiety is located in a pocket surrounded by Leuβ217, Leuβ219, Aspβ226, Hisβ229, and Leuβ230. Residues Valβ23, Alaβ233, Serβ236, and Pheβ272 generate a hydrophobic pocket occupied by the 3′-phenyl ring whereas the voluminous taxane ring is enclosed by the Proβ274, Leuβ275, Thrβ276, Serβ277, Argβ278, Proβ360, Argβ369, Glyβ370, and Leuβ371 residues. Furthermore, the phenyl ring of the 3′-benzamido group makes contact with Valβ23 and the oxetane oxygen participates in hydrogen bonding with the backbone N–H of Thrβ276 (Fig. 6C). Since dienone **8** is considerably smaller than paclitaxel, it is not able to fill the binding pocket to the same extent. However, the results suggest that the three different aromatic moieties in **8** are directed towards different hydrophobic regions in the paclitaxel binding site (Fig. 6B). The indole fragment is buried inside the hydrophobic pocket that binds to the 3′-phenyl ring in paclitaxel. The *N*′-benzyl moiety enters the same pocket as the 2-benzoyl phenyl group and the 3-bromo-5-chloro-2-hydroxyphenyl moiety is directed, via the alkene linker, down into a hydrophobic area which is surrounded by Proβ274, Thrβ276, Argβ278, Glnβ282, Argβ284, Leuβ286, and Leuβ371. Interestingly, the modeling study also suggested that **8** could interact via two hydrogen bonds with Thrβ276 (Fig. 6D): one between the phenolic hydrogen and the alcohol oxygen (2.31 Å, –OH···O 134°) and one hydrogen bond between the carbonyl oxygen and N–H in the protein backbone (2.14 Å, C═O···H–N 171°).

3. Conclusions

A series of dihalogenated chalcones and structurally related dienones have been synthesized using efficient methods. The compounds have been evaluated for their antiproliferative activity and for the effect on microtubule assembly. Several of the compounds showed cytotoxic activities (IC_{50} values in the low μM range) toward individual cancer cell lines. Five of the compounds were found to be tubulin polymerization inhibitors, and interestingly, one dienone derivative was found to stabilize tubulin to the same extent as the anticancer drug docetaxel. Tubulin inhibition was most favoured by compounds containing unsubstituted aromatic rings (i.e., phenyl or 2-thienyl as in **5** or **6**), an electron rich 4-diethylaminophenyl group (as in **1** and **2**) or an elongated styryl moiety in the 3-position of the chalcone structure (as in **7**). Stabilization of tubulin assembly was obtained in the presence of the significantly larger dienone structure **8** containing an additional aromatic moiety. Molecular docking studies suggested that the tubulin inhibitors bind into the colchicine binding site of β-tubulin while the novel tubulin-stabilizing agent seems to interact with the paclitaxel binding site. To the best of our knowledge, compound **8** is the first reported chalcone with microtubule-stabilizing activity, which could be a starting point for the development of novel small molecule microtubule-stabilizing agents.

4. Experimental

4.1. Chemistry

All reagents and solvents were of analysis or synthesis grade. ^1H and ^{13}C NMR-spectra were recorded on a JEOL JNM-EX 400-spectrometer at 400 and 100 MHz, respectively, in $CDCl_3$. Chemical shifts are reported in ppm with the solvent residual peak as internal standard ($CHCl_3$ δ 7.26, $CDCl_3$ δ 77.0). The reactions were monitored by thin-layer chromatography (TLC), on silica plated (Silica Gel 60 F_{254}, E. Merck), detecting spots by UV (254 and 365 nm). Melting points were measured in a Büchi Melting Point B-540 apparatus and were uncorrected. Elemental analyses were performed at Kolbe Mikroanalytisches Laboratorium, Mülheim and der Ruhr, Germany.

4.2. General procedure for the synthesis of chalcones 1–2

An aqueous solution of NaOH (60%, 25 mL/mmol acetophenone) was added dropwise to an ice-cooled solution of dihalogenated 2′-hydroxyacetophenone (1.0 equiv) and 4-diethylaminobenzaldehyde (1.3 equiv) in MeOH (25 mL/mmol acetophenone). The reaction was allowed to reach room temperature and was stirred over night. The reaction mixture was cooled to 0 °C and acidified with concd HCl (37%). The crude precipitate was filtered off, washed with water and recrystallized from EtOH.

4.2.1. (*E*)-1-(3-Bromo-5-chloro-2-hydroxyphenyl)-3-(4-diethylaminophenyl)prop-2-en-1-one (1)

3′-Bromo-5′-chloro-2′-hydroxyacetophenone (1.00 g, 4.0 mmol) gave **1** as red crystals (1.00 g, 62%). Mp: 153–154 °C; ^1H NMR ($CDCl_3$) δ 1.22 (t, J = 7.0 Hz, 6H), 3.44 (q, J = 7.0 Hz, 4H), 6.67 (d, J = 8.4 Hz, 2H), 7.28 (d, J = 14.3 Hz, 1H), 7.56 (d, J = 8.8 Hz, 2H), 7.69 (d, J = 1.5 Hz, 1H), 7.84 (d, J = 1.5 Hz, 1H), 7.97 (d, J = 15.0 Hz, 1H). The OH-signal was not observed in the spectrum, due to solvent exchange. ^{13}C NMR ($CDCl_3$) δ 12.6, 44.6, 111.3, 111.8, 112.7, 121.1, 121.4, 123.2, 127.8, 131.9, 137.7, 148.8, 150.6, 158.7, 191.7; IR: (KBr) ν 2963 (br), 1616, 1604, 1436, 1150 cm^{-1}. Anal. Calcd for $C_{19}H_{19}BrClNO_2$: C, 55.83; H, 4.69; N, 3.43. Found: C, 55.76; H, 4.73; N, 3.40.

4.2.2. (*E*)-1-(3,5-Dibromo-2-hydroxyphenyl)-3-(4-diethylaminophenyl)prop-2-en-1-one (2)

3′,5′-Dibromo-2′-hydroxyacetophenone (3.00 g, 10.2 mmol) gave **2** (3.59 g, 78%) as red crystals. Mp 137–141 °C; ^1H NMR ($CDCl_3$) δ 1.22 (t, J = 7.0 Hz, 6H), 3.44 (q, J = 7.0 Hz, 4H), 6.67 (d, J = 9.2 Hz, 2H), 7.22–7.31 (m, 1H), 7.56 (d, J = 8.8 Hz, 2H), 7.82 (d, J = 2.2 Hz, 1H), 7.92–8.01 (m, 2H), 12.87 (s, 1H). ^{13}C NMR ($CDCl_3$) δ 12.6, 44.6, 109.9, 111.3, 111.9, 113.1, 121.1, 122.1, 130.7, 131.9, 140.2, 148.8, 150.6, 159.2, 191.6; IR (KBr) ν 2966 (br), 1623, 1608, 1540, 1516, 1182, 1146 cm^{-1}. Anal. Calcd for $C_{19}H_{19}Br_2NO_2$: C, 50.36; H, 4.23; N, 3.09. Found: C, 50.31; H, 4.20; N, 2.96.

4.3. General procedure for the synthesis of chalcones 3–6 and dienones 7–8

KOH (2.9 equiv) was added to a solution of 3′-bromo-5′-chloro-2′-hydroxyacetophenone (1 equiv) and the appropriate aldehyde (1.05 equiv) in EtOH (6 mL/mmol acetophenone). The reaction was stirred at 50 °C for 3 h and was then allowed to reach room temperature over night. The reaction mixture was poured into water and acidified with aqueous HCl (1 M). The crude precipitate was filtered off.

4.3.1. (*E*)-1-(3-Bromo-5-chloro-2-hydroxyphenyl)-3-(4-(trifluoromethyl) phenyl)prop-2-en-1-one (3)

4-Trifluoromethylbenzaldehyde (2.19 g, 12.6 mmol) gave **3** (4.86 g, 98%), which could not be recrystallized from EtOH, due to instant cyclization upon heating. Mp 160 °C (decomp.). However, NMR spectrum and elemental analysis revealed that the crude precipitate had high purity; ^1H NMR ($CDCl_3$) δ 7.62 (d, J = 15.4 Hz, 1H), 7.72 (d, J = 8.5 Hz, 2H), 7.79–7.81 (m, 3H), 7.86 (d, J = 2.4 Hz, 1H), 7.98 (d, J = 15.4 Hz, 1H). The OH-signal was not observed in the spectrum, due to solvent exchange. ^{13}C NMR

($CDCl_3$) δ 113.3, 120.7, 121.3, 123.7 (q, $^1J_{CF}$ = 272.3 Hz), 123.9, 126.1 (q, $^3J_{CF}$ = 3.7 Hz), 128.1, 129.0, 132.8 (q, $^2J_{CF}$ = 32.9 Hz), 137.3, 139.1, 145.4, 158.8, 192.2. Anal. Calcd for $C_{16}H_9BrClF_3O_2$: C, 47.38; H, 2.24. Found: C, 47.28; H, 2.32.

4.3.2. (*E*)-1-(3-Bromo-5-chloro-2-hydroxyphenyl)-3-(4-methoxyphenyl)prop-2-en-1-one (4)

The crude precipitate was recrystallized from EtOH. *p*-Anisaldehyde (1.7 g, 12.6 mmol) gave **4** (3.9 g, 90%) as a yellow powder. Mp 167–168 °C; ^{1}H NMR ($CDCl_3$) δ 3.88 (s, 3H), 6.97 (d, *J* = 8.6 Hz, 2H), 7.43 (d, *J* = 15.3 Hz, 1H), 7.66 (d, *J* = 8.6 Hz, 2H), 7.74 (d, *J* = 2.2 Hz, 1H), 7.86 (d, *J* = 2.2 Hz, 1H), 7.97 (d, *J* = 15.3 Hz, 1H). The OH-signal was not observed in the spectrum, due to solvent exchange. ^{13}C NMR ($CDCl_3$) δ 55.5, 113.0, 114.6, 116.1, 121.0, 123.6, 126.8, 128.0, 131.0, 138.4, 147.5, 158.8, 162.6, 192.2. Anal. Calcd for $C_{16}H_{12}BrClO_3$: C, 52.28; H, 3.29. Found: C, 52.35; H, 3.25.[14]

4.3.3. (*E*)-1-(3-Bromo-5-chloro-2-hydroxyphenyl)-3-phenylprop-2-en-1-one (5)

The crude precipitate was recrystallized from EtOH. Benzaldehyde (0.45 g, 4.2 mmol) gave compound **5** (1.3 g, 96%). Mp 128–129 °C; ^{1}H NMR ($CDCl_3$) δ 7.47–7.50 (m, 3H), 7.57 (d, *J* = 15.4, 1H), 7.70–7.72 (m, 2H), 7.78 (d, *J* = 2.2 Hz, 1H), 7.88 (d, *J* = 2.2 Hz, 1H), 8.01 (d, *J* = 15.4 Hz, 1H), 13.51 (s, 1H). ^{13}C NMR ($CDCl_3$) δ 113.3, 119.0, 121.1, 124.0, 128.4, 129.2, 129.4, 131.8, 134.3, 139.0, 147.9, 159.0, 192.7.[14]

4.3.4. (*E*)-1-(3-Bromo-5-chloro-2-hydroxyphenyl)-3-(thiophen-2-yl)prop-2-en-1-one (6)

The crude precipitate was recrystallized from EtOH. 2-Thiophenecarboxaldehyde (0.47 g, 4.2 mmol) gave **6** (1.35, 96%). Mp 165–166 °C; ^{1}H NMR ($CDCl_3$) δ 7.15 (dd, *J* = 3.5, 5.0 Hz, 1H), 7.31 (d, *J* = 15.0 Hz, 1H), 7.46 (d, *J* = 3.5 Hz, 1H), 7.54 (d, *J* = 5.0 Hz, 1H), 7.76 (d. *J* = 2.3 Hz, 1H), 7.82 (d, *J* = 2.3 Hz, 1H), 8.12 (d, *J* = 15.0 Hz, 1H). The OH-signal was not observed in the spectrum, due to solvent exchange. ^{13}C NMR ($CDCl_3$) δ 113.0, 117.4, 120.8, 123.7, 128.0, 128.8, 130.7, 133.8, 138.6, 139.7, 139.9, 158.8, 191.9.[14]

4.3.5. (2*E*,4*E*)-1-(3-Bromo-5-chloro-2-hydroxyphenyl)-5-phenylpenta-2,4-dien-1-one (7)

The crude precipitate was recrystallized from EtOH. Cinnamic aldehyde (1.59 g, 12 mmol) gave **7** (3.45 g, 95%) as a yellow powder. Mp 148–149 °C; ^{1}H NMR ($CDCl_3$) δ 7.06–7.15 (m, 3H), 7.37–7.42 (m, 3H), 7.52–7.54 (m, 2H), 7.74–7.81 (m, 3H), 13.59 (s, 1H). ^{13}C NMR ($CDCl_3$) δ 113.1, 120.9, 122.1, 123.7, 126.4, 127.7, 128.1, 129.1, 130.0, 135.7, 138.6, 144.6, 147.6, 158.8, 192.4.

4.3.6. (2*E*,4*E*)-1-(3-Bromo-5-chloro-2-hydroxyphenyl)-5-(1-benzyl-1*H*-indol-3-yl)penta-2,4-dien-1-one (8)

The crude precipitate was recrystallized from EtOH. (*E*)-3-(1-Benzyl-1*H*-indol-3-yl)acrylaldehyde (0.82 g, 3.13 mmol) gave **8** (0.39 g, 26%) as a red powder. Mp 180 °C (decomp.); ^{1}H NMR ($CDCl_3$) δ 5.34 (s, 2H), 6.99–7.21 (m, 4H), 7.24–7.39 (m, 7H), 7.43 (s, 1H), 7.71 (d, *J* = 2.3 Hz, 1H), 7.80–7.89 (m, 2H), 7.96–8.00 (m, 1H). The OH-signal was not observed in the spectrum, due to solvent exchange. ^{13}C NMR ($CDCl_3$) δ 50.5, 77.2, 110.6, 112.8, 114.5, 116.1, 118.2, 120.7, 121.7, 122.7, 123.4, 126.1, 127.0, 127.9, 128.2, 129.0, 132.0, 136.0, 137.8, 138.0, 139.0, 150.0, 158.7, 192.0; HRMS (FT-ICR-MS): $[M+H]^+$ calcd for $C_{26}H_{19}BrClNO_2$, 492.0361. Found: 492.0363.

4.4. (1*Z*,4*E*)-1-(3-Bromo-5-chloro-2-hydroxyphenyl)-1-hydroxy-5-phenylpenta-1,4-dien-3-one (9)

trans-Cinnamoyl chloride (4.00 g, 24.0 mmol) was added to a solution of 3′-bromo-5′-chloro-2′-hydroxyacetophenone (5.00 g, 20.0 mmol) in dry pyridine (20 mL) and the reaction was stirred at room temperature for 48 h. Ice-water was added and the precipitate was filtered off. Recrystallization from EtOH (reflux) gave the esterified acetophenone as white crystals (6.63 g, 87%). Anhydrous K_2CO_3 (4.21 g, 30.48 mmol) was added to a solution of the esterified acetophenone (4.63 g, 12.19 mmol) in 2-butanone (125 mL) and the reaction was refluxed for 3.5 h. The reaction mixture was neutralized (pH 7) with concentrated AcOH and water was added. The precipitate was filtered off. Recrystallization from MeOH (reflux, 1 h) gave **9** as yellow crystals (3.40 g, 73%). Mp 154–155 °C; ^{1}H NMR ($CDCl_3$) δ 6.25 (s, 1H), 6.61 (dd, *J* = 1.2, 15.8 Hz, 1H), 7.38–7.45 (m, 3H), 7.53–7.59 (m, 2H), 7.61–7.65 (m, 1H), 7.67–7.70 (m, 1H), 7.73 (s, 1H), 12.93 (s, 1H). The enolate signal was not observed in the spectrum, due to solvent exchange. ^{13}C NMR ($CDCl_3$) δ 96.6, 113.1, 120.1, 121.4, 123.9, 127.0, 128.2, 129.0, 130.5, 134.6, 137.9, 141.4, 157.7, 176.0, 193.7. Anal. Calcd for $C_{17}H_{12}BrClO_3$: C, 53.78; H, 3.19. Found: C, 53.99; H, 3.51.

4.5. Biology

4.5.1. Cell lines

A panel of human cancer cell lines was used for the cytotoxicity studies. The panel has previously been described and consists of the parental sensitive cell lines: RPMI 8226 (myeloma), CCRF-CEM (leukemia), U937-GTB (lymphoma) and NCI-H69 (small-cell lung cancer) and the drug resistant sublines 8226/Dox40 (doxorubicin resistant myeloma), 8226/LR5 (melphalan resistant myeloma), CEM/VM1 (teniposide resistant leukemia), U937/Vcr (vincristine resistant lymphoma), H69AR (doxorubicin resistant small-cell lung cancer), and the primary resistant ACHN (renal adenocarcinoma) cell line.[28] This panel has been designed to represent different histologies as well as different mechanisms of drug resistance.[28] The cells were cultivated in complete cell medium consisting of culture medium RPMI 1640 supplemented with 10% heat-activated fetal calf serum, 2 mM glutamine, 100 μg/mL streptomycin and 100 U/mL penicillin (all purchased from Sigma–Aldrich, Stockholm, Sweden). The cells were grown in 37 °C in a humidified atmosphere containing 5% CO_2 and harvested in log-phase for experimental use.

4.5.2. Cytotoxicity studies

The cytotoxicity study was performed using the fluorometric microculture cytotoxicity assay (FMCA) method. FMCA is a total cell kill assay, based on the ability of cells with intact cell membranes to convert non-fluorescent fluorescein diacetate (FDA; Sigma–Aldrich) to fluorescent fluorescein.[19] The details of the method have been presented previously in the literature.[20] The cell suspensions (10,000–20,000 cells per mL) were exposed, at 37 °C, to varying concentrations of the test substances **1**–**9** (0.016, 0.08, 0.04, 2, 10, and 50 μM dissolved in DMSO with maximum 1% DMSO in cell suspensions) in 96-well microtiter plates (NUNC Brand Products, Denmark) for 72 h. Each compound concentration was tested in duplicate and the experiments were repeated twice. The cells were washed with phosphate-buffered saline (PBS) followed by the addition of FDA (dissolved in DMSO and diluted with physiological buffer to 10 μg/mL). The fluorescence was measured after 40 min incubation at 485/520 nm in a fluorometer (Fluorostar Optima, BMG Technologies; Germany). The fluorescence is proportional to the number of living cells, and the results were presented as survival index (fraction of surviving cells vs un-treated control wells). Log IC_{50} values (inhibitory concentration 50%) were calculated from the obtained data from log-concentration-effect curves in Graph Pad Prism (GraphPad software Inc., CA, USA) using non-linear regression analysis.

4.5.3. Tubulin polymerization assay

Effects on tubulin polymerization were monitored using a commercial kit (Tubulin Polymerization Assay Kit (Porcine tubulin and Fluorescence based), Cytoskeleton Inc., Denver, CO, USA), which utilize fluorescent reporter enhancement (the standard assay protocol was used).[29,30] The fluorescence was measured using FLUOstar OPTIMA and the test substances **1**–**9** (dissolved in DMSO) were evaluated at 5 and 25 μM. The experiment was performed twice (mean values are presented). Docetaxel (Apoteket AB, Sweden) and vincristine (Apoteket AB, Sweden) were used as positive stabilizing and destabilizing controls, respectively. Docetaxel and vincristine were diluted with PBS and used in the concentration of 3 μM.

4.6. Molecular modeling

Molecular modeling was performed using the Schrödinger Package, MAESTRO interface version 9.0 (r211). The structure of tubulin in complex with podophyllotoxin (PDB 1SA1) and the structure of tubulin in complex with taxol (PDB 1JFF) was utilized for the study.[24,25,27,31] Tubulin, chains A and B, together with the ligand were extracted and missing residues in the protein were added by the Prime application v. 2.1 (r211). The tubulin structure and the test compounds (**1**–**9**) were prepared and energy minimized according to standard procedure (e.g., ligand preparation). Docking was performed by using GLIDE v. 5.5 (r211) with extra precision (XP) settings and standard parameters for ligand docking. Figure 2 was made from three different X-ray structures (PDB: 1SA1, 1JFF, and 1Z2B).

Acknowledgments

The authors thank the Knut and Alice Wallenberg Foundation, the Swedish Research Council (#621-2010-4846) and the Academy of Finland for the financial support.

References and notes

1. Edwards, M. L.; Stemerick, D. M.; Sunkara, P. S. *J. Med. Chem.* **1990**, *33*, 1948.
2. Loa, J.; Chow, P.; Zhang, K. *Cancer Chemother. Pharmacol.* **2009**, *63*, 1007.
3. Lee, S. H.; Sohn, D. H.; Jin, X. Y.; Kim, S. W.; Choi, S. C.; Seo, G. S. *Biochem. Pharmacol.* **2007**, *74*, 870.
4. Deng, J. X.; Sanchez, T.; Al-Mawsawi, L. Q.; Dayam, R.; Yunes, R. A.; Garofalo, A.; Bolger, M. B.; Neamati, N. *Bioorg. Med. Chem.* **2007**, *15*, 4985.
5. Dimmock, J. R.; Elias, D. W.; Beazely, M. A.; Kandepu, N. M. *Curr. Med. Chem.* **1999**, *6*, 1125.
6. Srinivasan, B.; Johnson, T. E.; Lad, R.; Xing, C. G. *J. Med. Chem.* **2009**, *52*, 7228.
7. Ducki, S. *Anti-Cancer Agents Med. Chem.* **2009**, *9*, 336.
8. Hadfield, J. A.; Ducki, S.; Hirst, N.; McGown, A. T. In *Progress in Cell Cycle Research*; Meijer, L., Jézéquel, A., Roberge, M., Eds.; Editions Life in Progress: New York, 2003; Vol. 5, pp 309–325.
9. Peyrot, V.; Leynadier, D.; Sarrazin, M.; Briand, C.; Rodriquez, A.; Nieto, J. M.; Andreu, J. M. *J. Biol. Chem.* **1989**, *264*, 21296.
10. Peyrot, V.; Leynadier, D.; Sarrazin, M.; Briand, C.; Menendez, M.; Laynez, J.; Andreu, J. M. *Biochemistry* **1992**, *31*, 11125.
11. Ducki, S.; Rennison, D.; Woo, M.; Kendall, A.; Chabert, J. F. D.; McGown, A. T.; Lawrence, N. J. *Bioorg. Med. Chem.* **2009**, *17*, 7698.
12. Go, M. L.; Wu, X.; Liu, X. L. *Curr. Med. Chem.* **2005**, *12*, 483.
13. Boumendjel, A.; Boccard, J.; Carrupt, P. A.; Nicolle, E.; Blanc, M.; Geze, A.; Choisnard, L.; Wouessidjewe, D.; Matera, E. L.; Dumontet, C. *J. Med. Chem.* **2008**, *51*, 2307.
14. Dahlén, K.; Wallen, E. A. A.; Grøtli, M.; Luthman, K. *J. Org. Chem.* **2006**, *71*, 6863.
15. Dyrager, C.; Friberg, A.; Dahlén, K.; Fridén-Saxin, M.; Börjesson, K.; Wilhelmsson, L. M.; Smedh, M.; Grøtli, M.; Luthman, K. *Chem. Eur. J.* **2009**, *15*, 9417.
16. Lawrence, N. J.; Patterson, R. P.; Ooi, L.-L.; Cook, D.; Ducki, S. *Bioorg. Med. Chem. Lett.* **2006**, *16*, 5844.
17. Desideri, N.; Conti, C.; Mastromarino, P.; Mastropaolo, F. *Antiviral Chem. Chemother.* **2000**, *11*, 373.
18. Doria, G.; Romeo, C.; Forgione, A.; Sberze, P.; Tibolla, N.; Corno, M. L.; Cruzzola, G.; Cadelli, G. *Eur. J. Med. Chem.* **1979**, *14*, 347.
19. Larsson, R.; Nygren, P. *Anticancer Res.* **1989**, *9*, 1111.
20. Lindhagen, E.; Nygren, P.; Larsson, R. *Nat. Protoc.* **2008**, *3*, 1364.
21. Sullivan, C. M.; Smith, D. M.; Matsui, N. M.; Andrews, L. E.; Clauser, K. R.; Chapeaurouge, A.; Burlingame, A. L.; Epstein, L. B. *Cancer Res.* **1997**, *57*, 1137.
22. Dimmock, J. R.; Kandepu, M. N.; Hetherington, M.; Quail, W. J.; Pungazhenthi, U.; Sudom, A. M.; Chamankhah, M.; Rose, P.; Pass, E.; Allen, T. M.; Halleran, S.; Szydlowski, J.; Mutus, B.; Tannous, M.; Manavathu, E. K.; Myers, T. G.; De Clercq, E.; Balzarini, J. *J. Med. Chem.* **1998**, *41*, 1014.
23. Pazdur, R.; Kudelka, A. P.; Kavanagh, J. J.; Cohen, P. R.; Raber, M. N. *Cancer Treat. Rev.* **1993**, *19*, 351.
24. http://www.pdb.org.
25. Ravelli, R. B. G.; Gigant, B.; Curmi, P. A.; Jourdain, I.; Lachkar, S.; Sobel, A.; Knossow, M. *Nature* **2004**, *428*, 198.
26. Kim, D. Y.; Kim, K. H.; Kim, N. D.; Lee, K. Y.; Han, C. K.; Yoon, J. H.; Moon, S. K.; Lee, S. S.; Seong, B. L. *J. Med. Chem.* **2006**, *49*, 5664.
27. Lowe, J.; Li, H.; Downing, K. H.; Nogales, E. *J. Mol. Biol.* **2001**, *313*, 1045.
28. Dhar, S.; Nygren, P.; Csoka, K.; Botling, J.; Nilsson, K.; Larsson, R. *Br. J. Cancer* **1996**, *74*, 888.
29. http://www.cytoskeleton.com/products/biochem/bk011.html.
30. Bonne, D.; Heusele, C.; Simon, C.; Pantaloni, D. *J. Biol. Chem.* **1985**, *260*, 2819.
31. MAESTRO [9.0], Schrödinger, LLC, Portland, 2009; GLIDE [2.1], Schrödinger, LLC, Portland, 2009.